interpretations of surficial ice melting (e.g., Costard et al., 2001; Christensen, 2003), and points to an intimate genetic relationship between ice-rich mantling deposits and mid-latitude gully development (Milliken et al., 2003; Head et al., 2008; Dickson and Head, 2009; Schon and Head, 2011a). Finally, recent near-infrared spectral reflectance observations of the seasonal stability of carbon dioxide ice deposits on the surface imply that near-surface water ice is modifying thermal inertia in mid-latitude regions (Vincendon et al., 2010). Collectively, these observations provide significant evidence in support of widespread and relatively young ice-rich mantling deposits that blanket mid- and high-latitudes (Head et al., 2011), but they do not constrain the absolute age of the deposits, or episodes of emplacement. Models of vapor diffusion (e.g., Mellon et al., 2004; cf., Bandfield, 2007) can characterize the present-day stability of buried ice, but also cannot directly shed light on the age or origin of buried ice deposits.

Table 1

Fig. (name)	Longitude (E)	Latitude	Diam. (km)	HiRISE Observation	Age (Ma) ($D > 8$ m)	# of craters counted	Count area[6] (km^2)
2 (Thila)[a]	155.6	18.1	5.4	PSP_009346_1985	23.1	2,790	4.2
3 (Naryn)[b]	123.3	14.9	3.9	PSP_002570_1950	2.1	3,169	4.5
4 (Dilly)[c]	157.2	13.3	2.1	PSP_010203_1935	34.4	6,675	18.9
7	150.6	−20.8	7.3	PSP_010032_1590	31.5	12,482	3.8
8	94.8	−23.9	4.3	PSP_008030_1560	18.1	4,355	6.0
9	49.4	−24.9	0.8	PSP_009983_1550	5.8	860	6.5
10	115.7	−25.8	6.9	PSP_007436_1540	62	10,710	3.3
11	127.1	−25.9	2.9	PSP_008543_1540	34.5	6,749	8.9
12	59.1	−27.4	6.5	ESP_014400_1525	7.9	865	12.6
13	108.9	−28	7.3	PSP_004008_1520	2.2	1,451	7.0
14 (Zumba)[d]	226.9	−28.7	2.9	PSP_003608_1510	0.7	1,197	46.0
15	163.1	−29.5	3.4	ESP_020752_1500	0.9	5,408	4.5
16	116.2	−32.2	1.8	ESP_020701_1475	26.8	4,834	2.9
17 (Gasa)[e]	129.4	−35.7	7.0	PSP_004060_1440	1.2	289	6.8
5	46.4	−55.6	2.2	PSP_007030_1240	0.7	129	5.0
6	345.4	−77.9	1.4	ESP_013968_1020	0.3	332	15.1

[6]Count areas are variable due to factors including the extent of near-rim ejecta deposits, pitted areas that were avoided, and local topography that could make recognition of small craters difficult.

[a] Tornabene et al. (2006).
[b] Tornabene et al. (2006); Hartmann et al. (2010).
[c] Tornabene et al. (2006).
[d] Tornabene et al. (2006); Hartmann et al. (2010).
[e] Schon et al. (2009b); Kolb et al. (2010); Schon and Head (2011b).

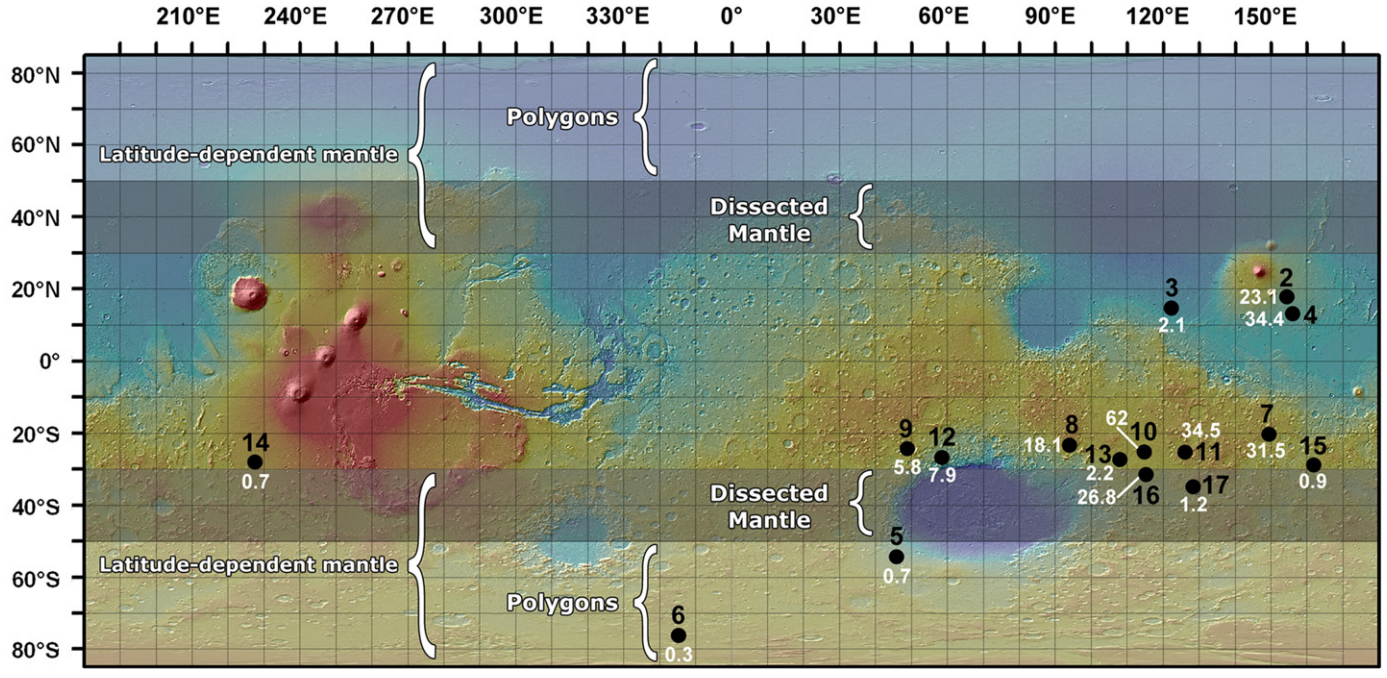

Fig. 1. Layers of ice-rich latitude-dependent mantling are found in both hemispheres (Head et al., 2003; 2011). Poleward of ~60° the terrain is dominated by patterned ground interpreted as contraction crack polygons. Between approximately 30 and 60°, where gullies and viscous flow features are commonly observed, the mantle is pitted, degraded, and partially removed. Dissected mantle refers to the remnant deposit of the former ice-rich dust layers. Equatorial rayed craters Thila (Fig. 2), Naryn (Fig. 3), and Dilly (Fig. 4) were identified by Tornabene et al. (2006). Additional young craters in this study occur in the polygonal terrain (Figs. 5 and 6) and bracket the equatorial extent of the mantle in the southern hemisphere (~30°S). Black numbers correspond to the associated figure. White numbers are crater-retention ages (Table 1). Background topography is from MOLA (red is high, blue is low). (For interpretation of the references to color in this figure legend, the reader is referred to the web version of this article.)